Petroleum Science (2018) 15:146–156
https://doi.org/10.1007/s12182-017-0204-z

ORIGINAL PAPER

Cover article

Fabrication of high-performance PVA/PAN composite pervaporation membranes crosslinked by PMDA for wastewater desalination

Rui Zhang[1] · Xiaoying Xu[1] · Bing Cao[1] · Pei Li[1]

Received: 17 July 2017 / Published online: 5 January 2018

Abstract
The pyromellitic dianhydride (PMDA) crosslinked poly(vinyl alcohol) (PVA) was coated on top of the PAN ultrafiltration membrane to form a PVA/PAN composite PV membranes for wastewater desalination. The composite membranes have high application value in industrial wastewater treatment. By varying the membrane fabrication parameters including the weight percent (wt%) of the PMDA, the crosslink temperature and duration, membrane with the best desalination performance was obtained. The composite membrane with a 2-μm-thick PVA selective layer containing 20 wt% of PMDA and being crosslinked at 100 °C for 2 h showed the highest NaCl rejection of 99.98% with a water flux of 32.26 L/(m^2 h) at 70 °C using the 35,000 ppm NaCl aqueous solution as feed. FTIR spectroscopy, wide-angle X-ray diffraction, thermogravimetric analysis and scanning electron microscope have been used to characterize the structures and properties of both the crosslinked PVA dense films and PVA/PAN composite membranes. The effects of the concentrations of PMDA, the crosslinking time and temperature to the membrane water contact angle, swelling degree, salt rejection and water flux were systematically studied.

Keywords Pervaporation · Desalination · Crosslinked PVA · Composite membranes · Wastewater treatment

1 Introduction

Water shortage has become a global issue that threats our daily life (Newman 1995; Wang et al. 2015). Wastewater desalination is considered as one of the most practical methods to solve this problem. Currently, reverse osmosis (RO) is the dominating technology due to its intrinsic advantages including: high salt rejection, good efficiency, easy to be operated, and energy-saving (Abufayed et al. 2003; Duong and Chung 2014; Sheikh et al. 2003). After a lot of RO saline water desalination plants have been built, environmental problem caused by the disposal of high concentrated brine water from the RO process has drew much attention to the public (Hou et al. 2017; Mitra et al. 2009; Yang et al. 2010; Yu et al. 2012). In our opinion, pervaporation (PV) technology provides a practicable solution to treat the brine water. The driving force of a PV process is the vapor pressure difference between the feed and permeate sides of the membrane. Theoretically, PV technology has the ability to treat high concentrated brine water as long as a low water vapor pressure in the permeate side can be maintained by applying vacuum in the membrane permeate side. Similar to membrane distillation (MD), phase transforming of the permeate is involved. However, the separation process of PV follows the solution-diffusion mechanism (Huang et al. 2001; Shao and Huang 2007). That is, the feed mixture first dissolves in the membrane feed side. Then, the permeates diffuse through the membrane and detach to the downstream side in a vapor state (Cheng et al. 2017; Das et al. 2011; Hong et al. 2011; Rachipudi et al. 2011; Xu et al. 2017; Zhang et al. 2009). Therefore, a PV membrane has a dense selective

Handling editor: Fanxing Li.

Edited by Xiu-Qin Zhu

✉ Bing Cao
Bcao@mail.buct.edu.cn

✉ Pei Li
lipei@mail.buct.edu.cn

[1] College of Materials Science and Engineering, Beijing University of Chemical Technology, Chaoyang District North Third Ring Road 15, Beijing 100029, China

layer which can mitigate the fouling problem encountered by a typical MD process where the pores of the MD membrane are easily fouled during the separation process. In the last decade, researchers start to study the feasibility of PV membranes for salty water desalination (Chaudhri et al. 2015; Cho et al. 2011b; Drobek et al. 2012; Liang et al. 2014, 2015; Wang et al. 2016b; Xie et al. 2011; Zwijnenberg et al. 2005).

Developing membrane materials with high permeability and selectivity is the key to fabricate high-performance PV membranes. Researchers mainly focus on synthesizing inorganic materials (Cho et al. 2011b; Drobek et al. 2012) or polymeric materials for the application of pervaporation desalination. The reported data demonstrate that both inorganic and polymeric PV membranes have high salt rejections but the water fluxes are relatively low (0.2–22.87 L/(m^2 h)) when separating a 1 wt% NaCl solution at 63 °C (Wang et al. 2016a; Xie et al. 2011; Zwijnenberg et al. 2005). Poly(vinyl alcohol) (PVA), with a super hydrophilicity and good film-forming ability, is an excellent polymeric material for PV. Since PVA is soluble in water, modification methods such as crosslink have to be used to increase its stability. Crosslinking PVA by small molecules is a straight forward way to increase PVA's stability. How to mitigate the decrease in water flux after crosslink reaction is the key of the selection of crosslinking method.

In this paper, the hydrolyzed PMDA was chosen as the crosslinked in the consideration of its stiff aromatic molecular structure and hydrophilic –COOH groups. After carrying out the esterification crosslink reaction between the –COOH group of the hydrolyzed PMDA and –OH group of PVA, the left unreacted –COOH group may act as the facilitate transport agent to water molecule, and the phenyl group in the PMDA molecule may increase the PVA fractional free volume (FFV) to benefit the water molecule diffusion. Therefore, the PMDA crosslinked PVA polymer may have high water flux as well as good stability in water. In order to improve the mechanical strength of the crosslinked PVA membrane, a PAN ultrafiltration membrane was adopted as the membrane substrate. Therefore, we fabricated a series of PVA/PAN composite pervaporation membranes. FTIR, TGA, DSC, WAXD, SEM and the swelling degree measurements were carried out to characterize the physiochemical properties of the composite membranes. And PV desalination tests were performed at different temperatures and NaCl concentrations to evaluate the separation performances of the prepared membranes.

2 Experimental

2.1 Materials

PVA-124 with a molecular weight (Mw) of 105,000 was purchased from Guoyao Chemical Reagent Co., Ltd (Beijing, China). The PAN ultrafiltration membranes with a molecular weight cutoff of 400 K were got from Ande Membrane Separation Technology and Engineering Co., Ltd (Beijing, China). PMDA with a purity >96% was bought from Aladdin Industrial Corporation (Shanghai, China). Sulfuric acid, sodium hydroxide and sodium chloride were obtained from Beijing Chemical Works. All chemicals were used without further purification.

2.2 Membrane preparation

The crosslinked PVA dense film and PVA/PAN composite membrane were prepared in the following procedures. First, prepare the PVA dope solutions. Specifically, 3 g of PVA was added in 100 mL deionized water. The mixture was stirred for at least 5 h at 90 °C to obtain a homogeneous solution. After the solution was cooled down to 70 °C, varied amount of PMDA was added and 2 drops of sulfuric acid were put in subsequently as a hydrolysis agent. Figure 1a shows the hydrolysis mechanism of the PMDA molecule in the presence of sulfuric acid. Then, the PVA solution was further stirred to ensure that all chemicals were totally dissolved. At last, the mixture was filtered and settled overnight to remove all non-dissolved particles and air bubbles.

The crosslinked PVA dense film was prepared by a solution-casting method. A 5-mL PVA dope solution was placed onto a PTFE plate. After being dried in air for 48 h at room temperature, a PVA film was formed and peeled off. The PVA dense film was heated at 100 °C for 2 h to carry out the crosslink reaction as shown in Fig. 1b and then used for characterizations including FTIR, TGA, DSC, WAXD, swelling degree and PV test.

To prepare the PVA/PAN composite membrane, a PAN ultrafiltration membrane was cut into a 6×6 cm square which was immersed in a 1.0 mol/L NaOH solution at 60 °C for 0.5 h to hydrolyze the PAN membrane surface. After that, the PAN membrane was soaked in deionized water several times to guarantee no alkali residue left in the membrane. Afterward, the PAN membrane was stick on a glass plate and the PVA/PAN composite membrane was obtained by the dip-coating method. Specifically, the PAN membrane was dipped into the 3 wt% PVA dope solution for 30 s. Then, the composite membrane was taken out and dried in air for 48 h at room temperature followed by heated at a predetermined temperature for certain period to

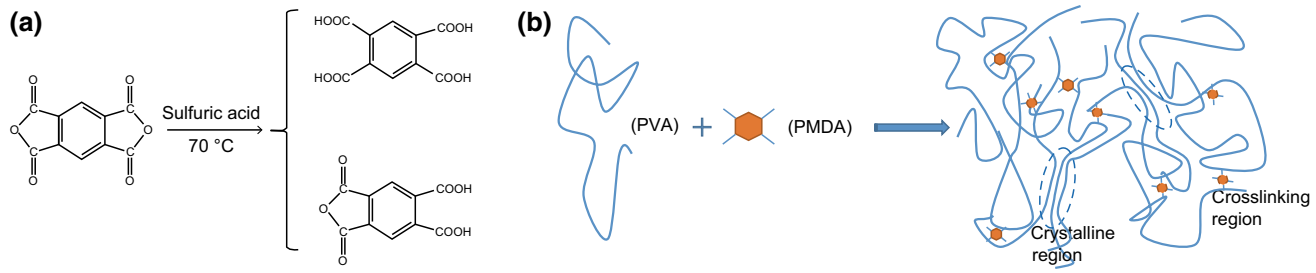

Fig. 1 **a** The hydrolysis mechanism of PMDA and **b** the PMDA crosslinked PVA diagram

perform the crosslink reaction. Using this method, the composite membrane with a 2-μm-thick PMDA crosslinked PVA coating layer were fabricated. The PVA layer with different amounts of PMDA crosslinkeds were denoted as: M-a, M-b, M-c, M-d, and M-e, respectively, corresponding to 0%, 5%, 10%, 20% and 30% of the mole concentrations of –COOH group of the hydrolyzed PMDA molecule to the –OH group of the PVA molecule.

2.3 Membrane characterization

2.3.1 Fourier transform infrared spectroscopy (FTIR)

An ATR-FTIR spectrometer (Spectrum RX I) purchased from PerkinElmer (USA) was used to confirmed the occurrence of the chemical reaction between the hydrolyzed PDMA and the PVA molecules. The dry PMDA crosslinked PVA films were placed on the sample holder, and the sample surface was scanned by the ATR-FTIR instrument. The frequency was set from 600 to 4000 cm^{-1} and the spectra were recorded with a resolution of cm^{-1}.

2.3.2 Wide-angle X-ray diffraction (WAXD)

The crystallinities of both the pure PVA and the PDMA crosslinked PVA films were investigated using a wide-angle X-ray diffractometer (D-8 advanced, Brucker's). The sample was first dried in vacuum for 24 h and then being scanned with a scanning rate of 0.3 °/min from 5° to 60°.

2.3.3 Thermal property analysis

Thermogravimetric analysis (TGA) of pure PVA and crosslinked PVA film samples were performed with a TA instruments Q500 at a heating rate of 10 °C/min from 30 to 800 °C under nitrogen. Differential scanning calorimetry (DSC) was performed on a TA Instruments Q20 calorimeter at a heating rate of 10 °C/min from 30 to 250 °C under nitrogen.

2.3.4 Scanning electron microscopy (SEM)

The surface and cross-sectional morphologies of PVA/PAN composite membranes were monitored by scanning electron microscope (S 4700, Hitachi). The samples were fractured in liquid nitrogen and coated with gold before test.

2.3.5 Water uptake and contact angle

The static water contact angles of all PVA dense films were measured by a contact angle meter (CAM200) at the room temperature. A 2 μL water drop was introduced onto the film surface for the contact angle measurement. At least three different locations of each sample were measured to get the average value of the water contact angle. The swelling degree of the films was measured based on the following procedure. The film samples were first vacuum-dried at room temperature overnight to obtain their dry weights W_d (g). Then, the dried samples were immersed in deionized water at room temperature till the swelling equilibriums were reached. After wipe off the spare water on the film surfaces, their weights W_s (g) were recorded. The swelling degree (S) of the films was calculated using Eq. (1):

$$S = \frac{W_s - W_d}{W_s} \times 100\% \quad (1)$$

Three repeated experiments were taken for each sample and the average result was recorded.

2.3.6 Pervaporation test

Pervaporation tests were carried out using a lab-made pervaporation unit presented in Fig. 2. The membrane with an effective surface area of 12.56 cm^2 was put in the membrane cell, and the pressure of the permeate side (downstream) was maintained at 100 Pa. The feed solutions with different NaCl concentrations range from 1 to 7 wt% were circulated using a peristaltic pump in the membrane feed side and their temperatures were maintained using a water bath. The permeate was collected by a

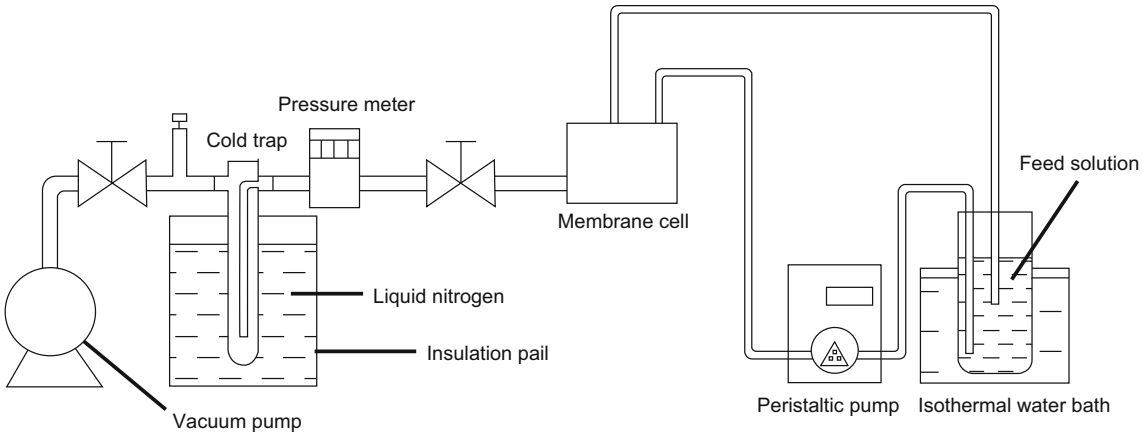

Fig. 2 The schematic diagram of the pervaporation unit

cold trap immersed in liquid nitrogen. The pervaporation tests were conducted at temperatures range from 30 to 70 °C, and at each condition the experiment was repeated for three times and the average value was recorded. Water flux (L/(m^2 h)) is determined using Eq. (2):

$$J = \frac{m}{A \times \mathrm{t}} \tag{2}$$

where m is the mass (or volume) of permeate, kg (or L); A is the effective membrane area, m^2; and t is the testing time, h. The salt concentrations of the feed and the permeate are determined by a conductivity meter (Oakton® Con 110) which is calibrated using standard NaCl solutions with different concentrations ranging from 0 to 100,000 ppm. A calibration curve is then constructed. The salt rejection R is calculated using Eq. (3):

$$R = \frac{c_\mathrm{f} - c_\mathrm{p}}{c_\mathrm{f}} \times 100\% \tag{3}$$

where c_f is the concentration of feed solution; and c_p is the concentration of the permeate. Membrane permeability P_i (Barrer) is calculated using Eq. (4) (Baker et al. 2010):

$$P_i = D_\mathrm{i} K_\mathrm{i} = j_i \frac{l}{P_{i0} - P_{il}} \tag{4}$$

where D_i is the diffusion coefficient of water, cm^2/s; K_i is the sorption coefficient of water, cm^3 (STP)/cm^{3}cmHg; P_{i0} and P_{il} are the water partial pressures on feed side and permeate side of the membrane; j_i is the molar flux, cm^3 (STP)/(cm^2 s).

3 Results and discussion

3.1 Membrane characterization

3.1.1 FTIR spectroscopy

Figure 3 shows the FTIR spectra of the pure PVA and crosslinked PVA films (M-a to M-e). All the films have characteristic peaks at 2800–3000 and 3320 cm^{-1}, representing the stretching vibrations of the C–H band and the O–H band in the PVA molecules (Rachipudi et al. 2011; Xie et al. 2011). As the PMDA concentration increases, more –OH groups of the PVA molecules react with the –COOH group of the hydrolyzed PMDA crosslinked, and the peak intensity of the O–H band (3320 cm^{-1}) gradually decreases. In addition, peaks at 1750 and 1275 cm^{-1}, which represent the C=O band and –C–O–C– band of aromatic ester, respectively, increase with the PMDA concentration. All the above-mentioned characteristic

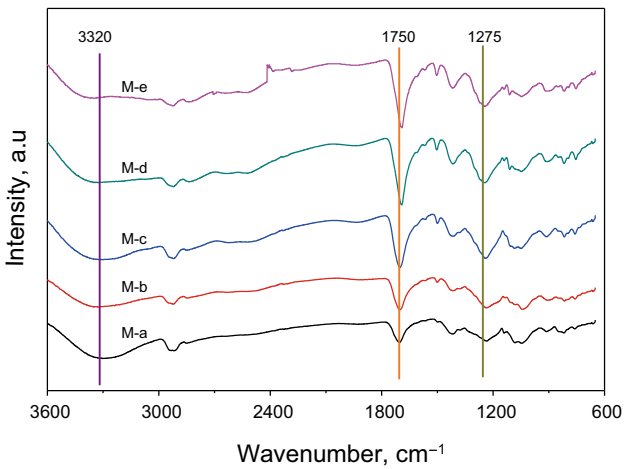

Fig. 3 FTIR spectroscopy of PVA dense films with different dosages of PMDA

peaks prove the occurrence of the crosslink reaction and the crosslinking degree increases with the concentration of PMDA.

3.1.2 TGA analysis

The effects of the PDMA crosslinked to the thermal stabilities of the PVA polymer are investigated using TGA. Figure 4 shows that all polymers show similar thermal degraded pattern. The first weight loss below 120 °C is attributed to the vaporization of the absorbed water in all polymers. In the temperature region of 120–250 °C, a 49.46% weight loss is observed for the pure PVA film which is identified as the decomposition of side chain and some amorphous carbons decomposition (Lai et al. 2015). For the crosslinked PVA, the weight loss in this region gradually decreases with the increase in the PMDA concentration. At the highest PMDA concentration (M-e), the weight loss reduces to 32.43%. This phenomenon indicates that the crosslink reaction significantly increases the thermal stability of PVA. The last weight loss region between 300 and 600 °C is probably relative to decomposition of the polymer backbones. Compared with the 27.2% weight loss of the pure PVA, the weight loss of M-e is only 11.26%. Again, this result indicates a better thermal stability of the PMDA crosslinked PVA polymer.

3.1.3 WXRD

Figure 5 shows the WXRD patterns for the pure PVA and crosslinked PVA films. All polymers have one diffraction peak with a 2θ value of 20°, which presents the crystalline domains of PVA (Liang et al. 2014). For pure PVA, the peak is very sharp and strong indicating its high crystallinity. But for the crosslinked PVA, the peak becomes

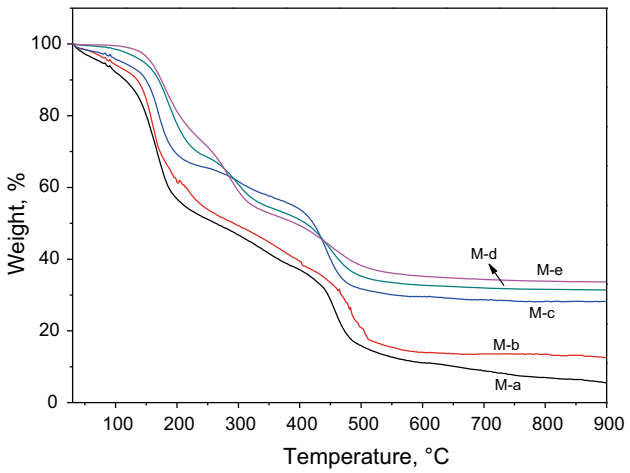

Fig. 4 Thermogravimetric analysis of pure PVA and crosslinked PVA films

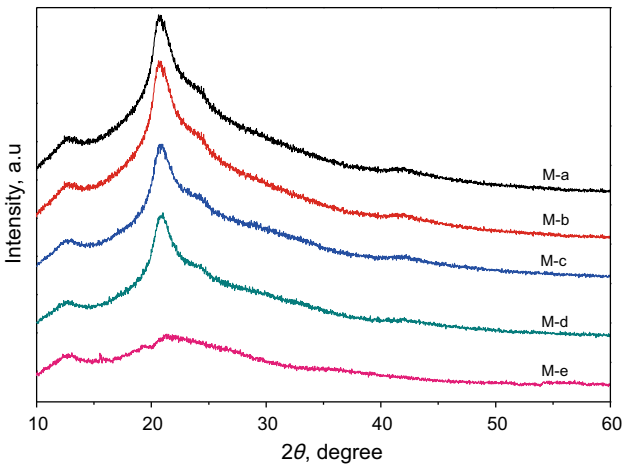

Fig. 5 Wide-angle X-ray diffraction patterns of pristine PVA and PMDA crosslinked membranes

weaker and broader as the crosslinking degree increases. For the pure PVA, the presence of large amounts of –OH groups and the flexible PVA polymer chains result in high crystalline degree. As the crosslinking degree increases, more and more –OH groups react with the –COOH groups of the PMDA crosslinked and the crosslinked PVA polymer chains are less flexible. Hence, it is difficult for the crosslinked PVA polymer chains to pack and form crystal regions. And the less crystal domains of the crosslinked PVA polymer shall benefit the water transport, since the crystal regions are impermeable to any penetrant.

3.1.4 DSC

According to Fig. 6, the pure PVA polymer has a glass transition temperature (T_g) around 75 °C. As the crosslinking degree increases, the glass transition region becomes less prominent and disappears for M-d and M-e. This indicates that the nature of the PVA polymers gradually turn from thermal plastic to thermal set material with the increase in crosslinking degree. The DSC curves also show that the melting temperature (T_m) of all polymers decreases from 223 °C of M-a to 175 °C of M-e and the melting peaks decrease as the crosslinking degree increases. This is in accordance with the WAXD results. Recall that, the crystallinity of highly crosslinked PVA polymer is low. Therefore, the less and small PVA crystals are easily melt and it leads to a lower melting temperature and smaller melting peak of the crosslinked PVA (Rachipudi et al. 2011).

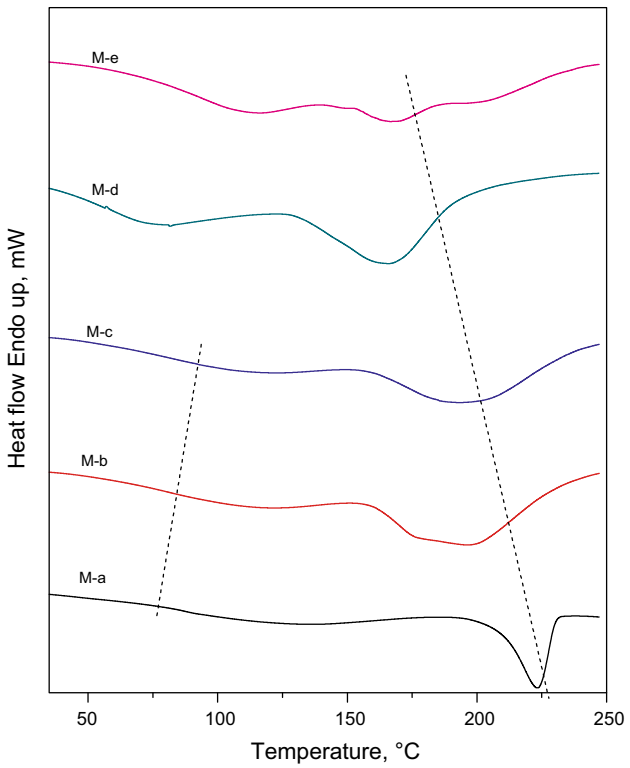

Fig. 6 The DSC curves of the pure PVA and PMDA crosslinked films (dash lines are to guide eyes)

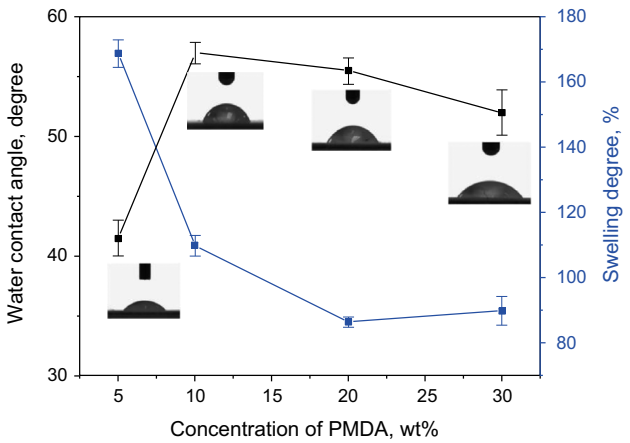

Fig. 7 The water contact angle and swelling properties of PVA films with different contents of PMDA

3.1.5 Effects of PMDA content on water uptake and water contact angle of the PVA films

Figure 7 shows the water contact angles and swelling degrees of all crosslinked PVA films. All films show a water contact angle less than 57° indicating their hydrophilic natures. When the concentration of PMDA increases from 5 to 10 wt% the water contact angle increases from 42.1° to 57.4° and the swelling degree decreases from 170.5% to 110.9%. This is due to that the –OH groups of the PVA polymer is consumed by the –COOH groups of the hydrolyzed PMDA molecule. Hence, the crosslinked PVA polymer is less hydrophilic and absorbs less water. With the concentration of PMDA increases further, more unreacted –COOH groups are left in the PVA film which leads to a slightly higher hydrophilicity. However, due to the increased crosslinking degree, the swelling degree continuously decreases to 90% for M-d (20% PMDA). As the concentration of PMDA increase to 30%, more and more unreacted –COOH groups increase the water contact angle of M-e to 52.5°. The higher hydrophilicity of the M-e film overplays the increased crosslinking degree. Therefore, the swelling degree slightly increases to 90%.

3.2 Morphology of the PVA/PAN composite membranes

The surface and cross-sectional morphologies of PAN ultrafiltration membrane and PVA/PAN composite membrane with 20% PMDA crosslinked are shown in Fig. 8. The cross section of the PAN ultrafiltration membrane has large finger-like micro-voids underneath the skin layer which can efficiently cut down the mass-transfer resistance of water vapor during the pervaporation desalination process. Besides, the top surface of the PAN membrane (Fig. 8b) has many pores in sizes of 10–20 nm which are formed after the hydrolysis treatment. These pores will allow the water vapor to pass through the dense layer region of the PAN membrane and reduce the resistance of the PAN substrate. Figure 8c shows that the dense PVA layer has a thickness of 1.8–2 μm, and Fig. 8d indicates that the PVA layer is defect free which can ensure a high salt rejection of the composite membrane.

3.3 Pervaporation performance

3.3.1 The effect of the content of PMDA to the separation performance of the dense PVA films

The pervaporation desalination performances of the crosslinked PVA films with different PMDA contents are studied. As shown in Table 1, all films show similar high salt rejections (99.9%). As the PMDA content increases from 5 to 20 wt%, the water flux increases from 9.88 to 16.47 L/(m^2 h). However, as the PMDA content further increases to 30%, the water flux reduces to 16.02 L/(m^2 h). The increase in the water flux might be due to that more unreacted –COOH groups left in the PVA film as the PMDA content increases to 20%. The –COOH groups act as the facilitate transport agent to water molecules and result in an increase in the water flux. However, as the PMDA concentration increases to 30%, the higher

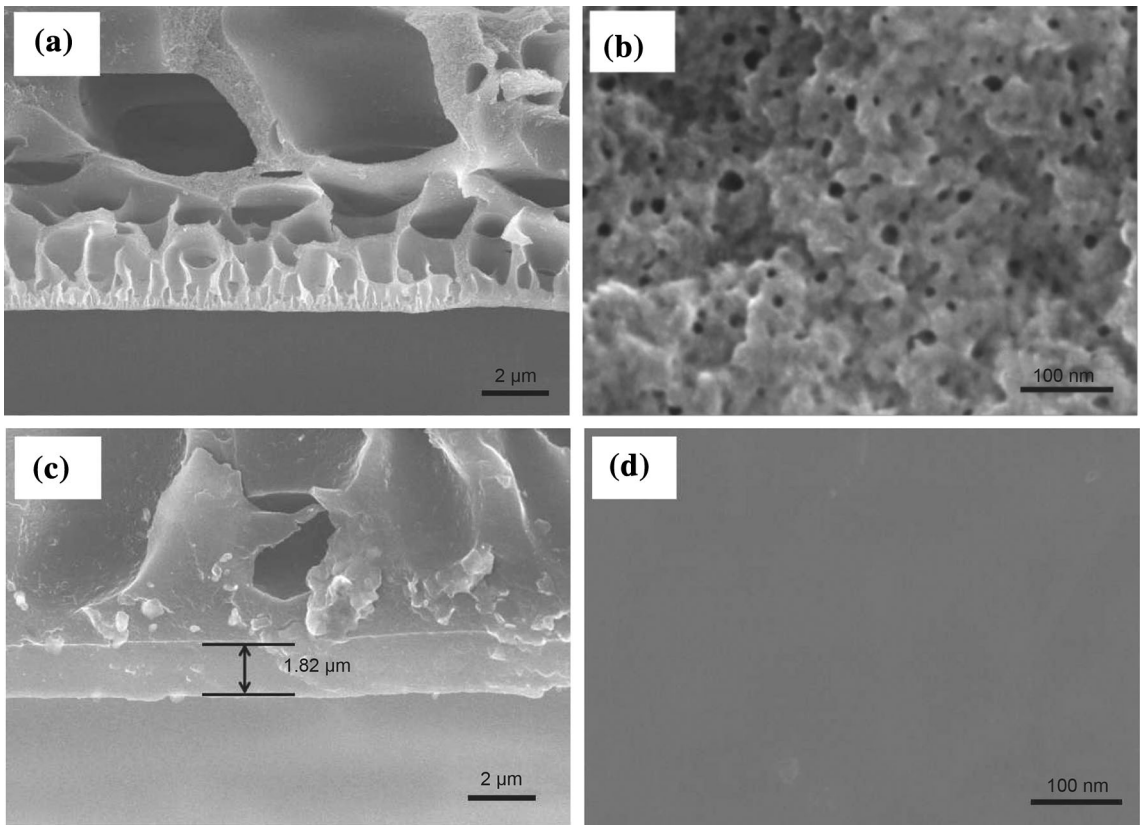

Fig. 8 SEM images of cross section (**a**) and top surface (**b**) of the PAN ultrafiltration membrane, and of the cross section (**c**) and surface (**d**) of the PVA/PAN composite membrane (M-d)

Table 1 Pervaporation performance of PMDA crosslinked PVA dense membranes at 50 °C using 35,000 ppm NaCl as the feed solution

	Flux, L m^{-2} h^{-1}	Permeability, 10^5 barrer	Rejection, %
M-b	9.88	1.50	99.96
M-c	12.32	1.87	99.98
M-d	16.47	2.51	99.98
M-e	16.02	2.47	99.98

crosslinking degree may reduce the chain flexibility of the PVA polymer and hence the water flux decreases. Since M-d has the highest water flux and salt rejection, the best concentration of PMDA crosslinker is selected to be 20 wt% for fabricating PVA/PAN composite membranes.

3.3.2 The effects of the crosslinking temperature and reaction time to the separation performance of composite membranes

In this study, PVA is crosslinked by the hydrolyzed PMDA crosslinked via the esterification reaction between the –COOH and –OH groups. The reaction rate of the esterification shall be boosted at higher temperatures. Insufficient crosslinked PVA membrane may result in low salt rejection since the un-crosslinked PVA is soluble in water. But over crosslinked PVA membrane may lead to low water flux due to that the highly inflexible PVA chain structure hinders the diffusion of water molecules. Therefore, it is important to figure out the most suitable crosslink temperature to obtain the composite membrane with sufficiently high salt rejection and good water flux. Figure 9a shows the water contact angles and the swelling degrees of the M-d dense films crosslinked at different temperatures from 70 to 140 °C for 2 h. Figure 9b shows the desalination performance of the corresponding PVA/PAN composite membranes crosslinked at the same temperatures. As the crosslink temperature increases from 70 to 100 °C, the water contact angle slightly increases from 33.2° to 39.4° but the swelling degree significantly decreases from 106.4% to 87.3%. This indicates that the crosslink reaction is more completed at 100 °C than at 70 °C, and that the water flux reduces from 35 to 32 L/(m^2 h) indicates that highly crosslinked PVA structure hinders the diffusion of water molecules. Note that, the salt rejection of the PVA/PAN composite membrane crosslinked at 70 °C is below

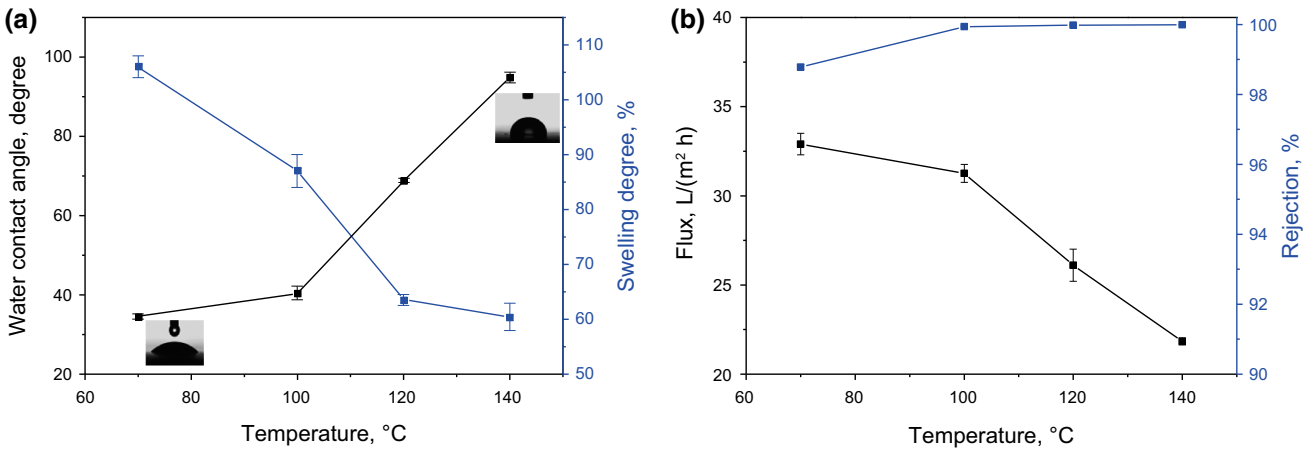

Fig. 9 **a** The water contact angles and swelling properties and **b** the water flux and salt rejections (using the 35,000 ppm NaCl solution as the feed at 70 °C) of M-d composite membranes crosslinked at different temperatures for 2 h

99%. When the crosslinked temperature increases to 100 °C, the salt rejection is higher than 99.95%. Therefore, the crosslink temperature needs to reach 100 °C to ensure an efficient salt rejection. With the further increases in the crosslink temperature, both the membrane swelling degrees and the water fluxes significantly decrease. Since increases the crosslink temperature from 100 to 140 °C just reduces the water flux from 32 to 22 L/(m^2 h). The best crosslink temperature is selected at 100 °C.

Similar to the crosslink temperature, the crosslink time also determine the degree of the crosslinking of the PVA membrane which influences the desalination property. Figure 10a shows that the water contact angles and swelling degrees change from 35.5° to 89.8°, and 118.6% to 51.3%, respectively, as the crosslink time gradually increases to 24 h. The phenomena indicate the esterification reaction continues with time and the resulting PVA films become less hydrophilic. Figure 10b shows that the crosslink time needs to be at least 2 h to ensure a salt rejection higher than 99.95%. And further increase in the crosslink time only reduces the water flux. Therefore, the best crosslink time for M-d composite membrane is selected at 2 h.

3.3.3 The effects of the NaCl concentration and temperature of the feed solution to the separation performance

Figure 11a shows that the water flux increases with temperature and decreases with the increase in the NaCl concentration of the feed solution. The increase in the water flux can be explained by the increases in the saturate water vapor pressure in the membrane feed side and the increase in the diffusivity of the water molecule in the membrane. Note that the driving force of PV process is the vapor pressure difference between the membrane feed and

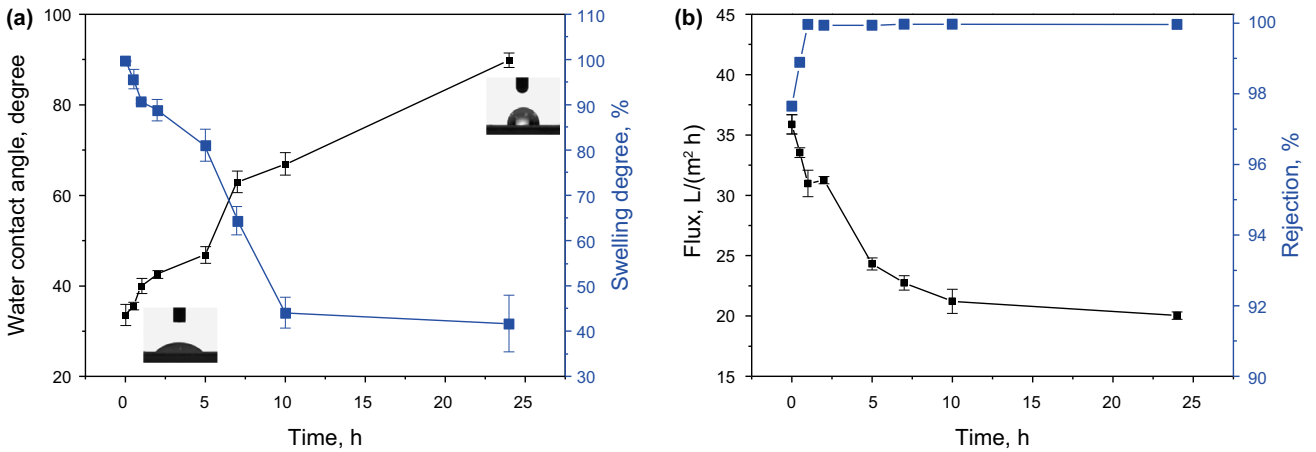

Fig. 10 The effect of crosslink time on **a** water contact angles and swelling degrees of M-d film and **b** water flux and salt rejections of M-d composite membranes

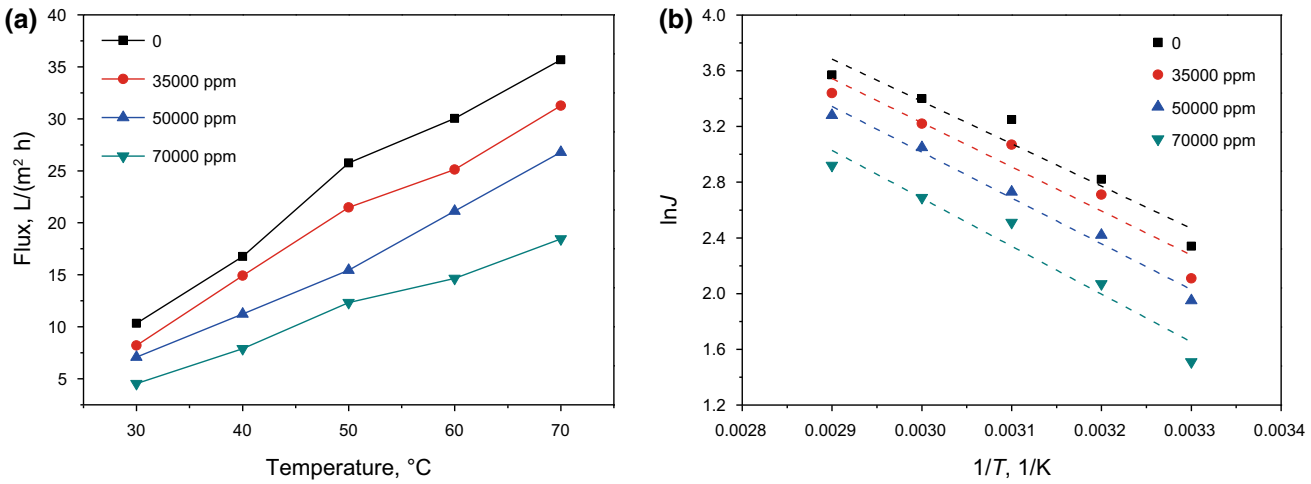

Fig. 11 **a** The relations of water flux to the NaCl concentration and temperature of the feed of the M-d composite membrane crosslinked for 2 h at 100 °C; **b** the Arrhenius plots of the water flux and the feed temperature at different NaCl concentrations

permeate side and the saturate water vapor pressure is in exponentially proportional to the temperature in the unit of kelvin of the feed solution. Therefore, when the temperature of the feed solution increases from 30 to 70 °C, the driving force of the water transport shall dramatically increase. In addition, transport in PV process follows the solution-diffusion mechanism where the diffusivity is governed by the size of the penetrant, polymer free volume and polymer chain flexibility. As the temperature increases, the PVA polymer chain becomes more flexible that favors the diffusion of the water molecules. Therefore, the increases in both the driving force and the diffusivity of the water molecules lead to the significantly improved water flux. On the contrary to the effect of the temperature, the increase in the NaCl concentration shall decrease the water flux. The high NaCl content dilutes the water concentration so that the saturate water vapor pressure in the membrane feed side decreases. It reduces the driving force of the water molecule. Furthermore, at a high NaCl concentration, concentration polarization in the membrane feed side becomes more severe. This will further decrease the water concentration in the membrane feed side. Therefore, these two phenomena cause the water flux to decrease from 35.12 L/(m^2 h) for pure water to 18.02 L/(m^2 h) for the 70,000 ppm NaCl feed solution at 70 °C.

Figure 11b shows that the logarithmic membrane water fluxes are linearly correlated with the reciprocal temperatures of the feed solutions. This is well fit to the Arrhenius correlation as described in Eq. (5).

$$J_i = A_i \exp\left(-\frac{E_{p,i}}{RT}\right) \tag{5}$$

where A_i is pre-exponential factor; R is the gas constant; T is the absolute temperature and $E_{p,i}$ is the apparent activation energy for permeation and reflects the amount of the energy barrier when the component passes though the membrane. Table 2 shows the apparent activation energies calculated from the slop of Fig. 11b and compares it to the literature data. The water activation energies of feeds with different salt concentrations are very similar

Table 2 Pervaporation performance of different membranes

Material	NaCl, ppm	T, °C	Membrane thickness, μm	Flux, L m^{-2} h^{-1}	Rejection, %	Positive activation energy, kJ mol^{-1}
Poly(vinyl alcohol)/maleic anhydride/silica (Xie et al. 2011)	2000	65	10	11.7	99.9	23.8
Graphene oxide/polyacrylonitrile (Liang et al. 2015)	35,000	90	0.1	65.1	99.8	22.19
Polyether ester (Quiñones-Bolaños et al. 2005)	3200	22	160	0.16	–	44.3
Fluoroalkylsilane-ceramic (Kujawski et al. 2007)	30,000	40	23	5	–	51
NaA zeolite (Cho et al. 2011a)	35,000	69	–	1.9	99.9	–
PVA/PMDA (this study)	35,000	70	2	32.26	99.8	23.6

(23.6–24.3 kJ mol^{-1}) for the PVA/PAN composite membranes. The positive value of $E_{p,i}$ implies that water flux shall increase with the temperature of the feed solution (Wang et al. 2016a). According to Table 2, our PVA/PAN composite PV membrane exhibits the second highest water flux. The good performance can be attributed to two reasons. First, the activation energy of the PVA/PAN composite membrane is very low, which means that water molecules need less energy to diffuse through the membrane. Second, the dense layer thickness of the PVA/PAN composite membrane is only 2 μm which reduces the resistance to the mass transfer of the water molecule. Note that, the graphene oxide/polyacrylonitrile composite membrane with the thinnest dense layer thickness of 0.1 μm has the highest water flux of 65.1 L/(m^2 h). Therefore, the water flux of the PMDA crosslinked PVA/PAN composite membrane can be further increased by reducing the PVA layer thickness.

4 Conclusion

The PMDA crosslinked PVA dense films have been prepared. The PV experimental results show that both the water fluxes and NaCl rejections increase as the PMDA content in the PVA dense film increases. The facilitate transport –COOH group in the PMDA molecules can be account for the increase in the water flux and the crosslinked PVA structure improves the NaCl rejection. The dense PVA film containing 20% of PMDA exhibits the highest PV performance with a water flux of 16.47 L/(m^2 h) and a NaCl rejection of 99.98%. The PMDA crosslinked PVA/PAN composite PV membranes with high desalination performance have also been successfully fabricated. The PVA/PAN composite membrane with 20 wt% PMDA crosslinked at 100 °C for 2 h shows the best separation performance with a water flux of 32.26 LMH and a NaCl rejection of 99.98% using the 35,000 ppm NaCl solution as the feed solution and operated at 70 °C. The excellent desalination property indicates a great potential for the PMDA crosslinked PVA/PAN composite membrane for treating high concentrated NaCl solutions.

Acknowledgements The project is supported by the Higher Education and High-quality and World-class Universities (PY201618), the National Natural Science Foundation of China (Contract Grant Number 51373014) and the National Natural Science Foundation of China (Contract Grant Number 51403012).

References

Abufayed AA, Elghuel M, Rashed M (eds). Desalination: a viable supplemental source of water for the arid states of North Africa. In: Conference on desalination strategies in South Mediterranean Countries. 2003. https://doi.org/10.1016/S0011-9164(02)01050-0.

Baker RW, Wijmans JG, Yu H. Permeability, permeance and selectivity: a preferred way of reporting pervaporation performance data. J Membr Sci. 2010;348(1):346–52. https://doi.org/10.1016/j.memsci.2009.11.022.

Chaudhri SG, Rajai BH, Singh PS. Preparation of ultra-thin poly(vinyl alcohol) membranes supported on polysulfone hollow fiber and their application for production of pure water from seawater. Desalination. 2015;367:272–84. https://doi.org/10.1016/j.desal.2015.04.016.

Cheng X, Ding S, Guo J, Zhang C, Guo Z, Shao L. In-situ interfacial formation of TiO_2/polypyrrole selective layer for improving the separation efficiency towards molecular separation. J Membr Sci. 2017. https://doi.org/10.1016/j.memsci.2017.04.057.

Cho CH, Oh KY, Si KK, Yeo JG, Lee YM. Improvement in thermal stability of NaA zeolite composite membrane by control of intermediate layer structure. J Membr Sci. 2011a;366(1–2):229–36. https://doi.org/10.1016/j.memsci.2010.10.006.

Cho CH, Oh KY, Si KK, Yeo JG, Sharma P. Pervaporative seawater desalination using NaA zeolite membrane: mechanisms of high water flux and high salt rejection. J Membr Sci. 2011b;371(1–2):226–38. https://doi.org/10.1016/j.memsci.2011.01.049.

Das P, Ray SK, Kuila SB, Samanta HS, Singha NR. Systematic choice of crosslinker and filler for pervaporation membrane: a case study with dehydration of isopropyl alcohol–water mixtures by polyvinyl alcohol membranes. Sep Purif Technol. 2011;81(2):159–73. https://doi.org/10.1016/j.seppur.2011.07.020.

Drobek M, Yacou C, Motuzas J, Julbe A, Ding L, Costa JCDD. Long term pervaporation desalination of tubular MFI zeolite membranes. J Membr Sci. 2012;415–416(10):816–23. https://doi.org/10.1016/j.memsci.2012.05.074.

Duong PHH, Chung TS. Application of thin film composite membranes with forward osmosis technology for the separation of emulsified oil–water. J Membr Sci. 2014;452(3):117–26. https://doi.org/10.1016/j.memsci.2013.10.030.

Hong WU, Xianshi LI, Nie M, Ben LI, Jiang Z. Integral PVA-PES composite membranes by surface segregation method for pervaporation dehydration of ethanol. Chin J Chem Eng. 2011;19(5):855–62. https://doi.org/10.1016/s1004-9541(11)60065-7.

Hou D, Lin D, Zhao C, Wang J, Fu C. Control of protein (BSA) fouling by ultrasonic irradiation during membrane distillation process. Sep Purif Technol. 2017;175:287–97. https://doi.org/10.1016/j.seppur.2016.11.047.

Huang RYM, Shao P, Feng X, Burns CM. Pervaporation separation of water/isopropanol mixture using sulfonated poly(ether ether ketone) (SPEEK) membranes: transport mechanism and separation performance. J Membr Sci. 2001;192(1–2):115–27. https://doi.org/10.1016/s0376-7388(01)00539-7.

Kujawski W, Krajewska S, Kujawski M, Gazagnes L, Larbot A, Persin M. Pervaporation properties of fluoroalkylsilane (FAS)

grafted ceramic membranes. Desalination. 2007;205(1):75–86. https://doi.org/10.1016/j.desal.2006.04.042.

Lai D, Wei Y, Zou L, Xu Y, Lu H. Wet spinning of PVA composite fibers with a large fraction of multi-walled carbon nanotubes. Progr Nat Sci Mater Int. 2015;25(5):445–52. https://doi.org/10.1016/j.pnsc.2015.10.003.

Liang B, Pan K, Li L, Giannelis EP, Cao B. High performance hydrophilic pervaporation composite membranes for water desalination. Desalination. 2014;347(17):199–206. https://doi.org/10.1016/j.desal.2014.05.021.

Liang B, Zhan W, Qi G, Lin S, Nan Q, Liu Y, et al. High performance graphene oxide/polyacrylonitrile composite pervaporation membranes for desalination applications. J Mater Chem A. 2015;3(9):5140–7. https://doi.org/10.1039/c4ta06573e.

Mitra SS, Thomas AR, Guo TG. Evaluation and characterization of seawater RO membrane fouling. Desalination. 2009;247(1–3):94–107. https://doi.org/10.1016/j.desal.2008.12.016.

Newman A. Ranking pesticides by environmental impact. Environ Sci Technol. 1995;29(7):324A–6A. https://doi.org/10.1021/es00007a748.

Quiñones-Bolaños E, Zhou H, Soundararajan R, Otten L. Water and solute transport in pervaporation hydrophilic membranes to reclaim contaminated water for micro-irrigation. J Membr Sci. 2005;252(1):19–28. https://doi.org/10.1016/j.memsci.2004.10.038.

Rachipudi PS, Kariduraganavar MY, Kittur AA, Sajjan AM. Synthesis and characterization of sulfonated-poly(vinyl alcohol) membranes for the pervaporation dehydration of isopropanol. J Membr Sci. 2011;383(1–2):224–34. https://doi.org/10.1016/j.memsci.2011.08.040.

Shao P, Huang RYM. Polymeric membrane pervaporation. J Membr Sci. 2007;287(2):162–79. https://doi.org/10.1016/j.memsci.2006.10.043.

Sheikh RE, Ahmed M, Hamdan S. Strategy of water desalination in the Gaza Strip. Desalination. 2003;156(1):39–42. https://doi.org/10.1016/s0011-9164(03)00322-9.

Wang J, Shang Y, Wang H, Zhao Y, Yin Y. Beijing's water resources: challenges and solutions. Jawra J Am Water Resour Assoc. 2015;51(3):614–23. https://doi.org/10.1111/1752-1688.12315.

Wang Q, Li N, Bolto B, Hoang M, Xie Z. Desalination by pervaporation: a review. Desalination. 2016a;387:46–60. https://doi.org/10.1016/j.desal.2016.02.036.

Wang Q, Lu Y, Li N. Preparation, characterization and performance of sulfonated poly(styrene-ethylene/butylene-styrene) block copolymer membranes for water desalination by pervaporation. Desalination. 2016b;390:33–46. https://doi.org/10.1016/j.desal.2016.04.005.

Xie Z, Ng D, Hoang M, Duong T, Gray S. Separation of aqueous salt solution by pervaporation through hybrid organic–inorganic membrane: effect of operating conditions. Desalination. 2011;273(1):220–5. https://doi.org/10.1016/j.desal.2010.10.026.

Xu YC, Tang YP, Liu LF, Guo ZH, Shao L. Nanocomposite organic solvent nanofiltration membranes by a highly-efficient mussel-inspired co-deposition strategy. J Membr Sci. 2017;526:32–42. https://doi.org/10.1016/j.memsci.2016.12.026.

Yang HL, Huang CP, Chun-TeLin J. Seasonal fouling on seawater desalination RO membrane. Desalination. 2010;250(2):548–52. https://doi.org/10.1016/j.desal.2009.09.021.

Yu C, Wu J, Contreras AE, Li Q. Control of nanofiltration membrane biofouling by *Pseudomonas aeruginosa* using d-tyrosine. J Membr Sci. 2012;423–424(51):487–94. https://doi.org/10.1016/j.memsci.2012.08.051.

Zhang W, Zhang Z, Wang X. Investigation on surface molecular conformations and pervaporation performance of the poly(vinyl alcohol) (PVA) membrane. J Colloid Interface Sci. 2009;333(1):346. https://doi.org/10.1016/j.jcis.2009.01.058.

Zwijnenberg HJ, Koops GH, Wessling M. Solar driven membrane pervaporation for desalination processes. J Membr Sci. 2005;250(1–2):235–46. https://doi.org/10.1016/j.memsci.2004.10.029.